CrossMark

RESEARCH ARTICLE

Finite Element Model to Study Calcium Distribution in T Lymphocyte Involving Buffers and Ryanodine Receptors

Hemant Kumar[1] · Parvaiz Ahmad Naik[2] · Kamal Raj Pardasani[3]

Abstract In this paper an attempt has been made to develop a mathematical model to study intracellular calcium distribution in T lymphocyte for a one dimensional unsteady state case. The model incorporates the parameters like diffusion coefficient, ryanodine receptors (RyRs), source influx and buffers. The boundary conditions have been framed using biophysical conditions of the problem. The finite element method has been employed to obtain the solution of the proposed mathematical model. The numerical results are used to study relationship between concentration and position with respect to source influx, buffers and ryanodine receptors (RyRs).

Keywords Finite element method · Buffers · MATLAB · T lymphocytes · Ryanodine receptors (RyRs) · Diffusion coefficient · Reaction diffusion equations

1 Introduction

Calcium (Ca^{2+}) is a universal second messenger, found in almost all cell types. Its intracellular level is regulated by finely tuned machinery responsible for calcium uptake, release, and intracellular storage. T lymphocytes are no exception in this regard. There are several calcium channels and transporters that play a key role in balancing cytoplasmic calcium levels in T lymphocytes. Pathways of calcium homeostasis participate in a number of cellular processes that determine short and long-term function of T lymphocytes. Therapeutic strategies are now evolving based on the modulation of T lymphocyte calcium homeostasis in order to combat immune—mediated disorders [1]. Ca^{2+} entry across the plasma membrane is the most important Ca^{2+} stores for T lymphocyte activation [2]. The ion channels that regulate calcium influx from the extracellular space in T lymphocytes either by conducting calcium ions or by modulating the membrane potential that provides driving force for calcium influx [3, 4]. The best characterized calcium channel in T lymphocytes is the calcium released-activated calcium (CRAC) channel, which is composed of ORAI and stromal interaction molecule (STIM) proteins [1]. The ORAI proteins and most prominently ORAI1 are the molecular basis for Ca^{2+} release-activated calcium (CRAC) channels. CRAC/ORAI1 channels are well defined through their biophysical and pharmacological properties [2].

Ca^{2+} dynamics [5] is the exchange of Ca^{2+} ions between intracellular Ca^{2+} stores and the cytosol, entering and leaving ions between the cells and binding activity of calcium and calcium binding proteins. The most important calcium binding proteins are itself buffers that are located in Ca^{2+} stores. The buffers bind more calcium molecules when the calcium concentration is higher in the cell [6, 7]. In T lymphocytes, the main buffer within cytosol is calmodulin (CaM) [8] with 4 calcium binding sites per CaM. There is a diversity of measured CaM concentrations depending on cell type and organ [8]. The binding of Ca^{2+} concentration to buffers serves as an indicator of free calcium concentration in intracellular measurements. Furthermore other second messengers derived from the adenine dinucleotides, nicotinamide adenine dinucleotide (NAD), and nicotinamide adenine dinucleotide

✉ Parvaiz Ahmad Naik
  naik.parvaiz@yahoo.com

1   Department of Mathematics, Indian Institute of Technology, Roorkee, Uttarakhand 247667, India

2   Department of Mathematics, Islamic University of Science & Technology, Awantipora, Jammu and Kashmir 192122, India

3   Department of Mathematics, Maulana Azad National Institute of Technology, Bhopal 462003, India

phosphate (NADP) have also been implicated in T lympho-cyte calcium signaling [9]. Nicotinic acid adenine dinu-cleotide phosphate (NAADP) acts as a very early second messenger upon TCR/CD3 engagement, while cyclic ADP-ribose (cADPR) is mainly involved in sustained partial depletion of the endoplasmic reticulum by stimulating cal-cium release via ryanodine receptors (RyRs) [1].

A good number of theoretical attempts [10–24] are reported in the literature for the study of calcium signaling in neuron cells, astrocytes, oocytes, acinar cells, fibroblasts, etc. But very few attempts are reported [2, 8, 25] for theo-retical study of calcium signaling in T lymphocytes. No attempt is reported in the literature for calcium diffusion based study of calcium signaling in T lymphocytes. In the present paper an attempt has been made to develop a model for intracellular calcium distribution in T lymphocyte involving calcium diffusion, buffers and influx of Ca^{2+} from ryanodine receptors (RyRs) channels. The model has been developed for a one dimensional unsteady state case. The finite element method has been used to obtain the solution.

2 Mathematical Formulation

Calcium kinetics in T lymphocytes is governed by a set of reaction–diffusion equations which can be framed assum-ing the following bimolecular reaction between Ca^{2+} and buffer species [17, 26–28]

$$[Ca^{2+}] + [B_j] \xrightleftharpoons[k_j^-]{k_j^+} [CaB_j] \tag{1}$$

where $[Ca^{2+}]$, $[B_j]$ and $[CaB_j]$ represent the cytosolic Ca^{2+} concentration, free buffer concentration and calcium bound buffer concentration respectively and 'j' is an index over buffer species, k_j^+ and k_j^- are 'on' and 'off' rates for jth buffer respectively. Using Fickian diffusion, the buffer reaction diffusion system in one dimension is expressed as [10, 11, 17, 26, 27]

$$\frac{\partial [Ca^{2+}]}{\partial t} = D_{Ca} \nabla^2 [Ca^{2+}] + \sum R_j \tag{2}$$

$$\frac{\partial [B_j]}{\partial t} = D_{B_j} \nabla^2 [B_j] + \sum R_j \tag{3}$$

$$\frac{\partial [CaB_j]}{\partial t} = D_{CaB_j} \nabla^2 [CaB_j] - \sum R_j \tag{4}$$

where reaction term R_j is given by

$$R_j = -k_j^+ [Ca^{2+}][B_j] + k_j^- [CaB_j] \tag{5}$$

D_{Ca}, D_{B_j}, D_{CaB_j} are diffusion coefficients of free calcium, free buffer and Ca^{2+} bound buffer respectively and σ_{RyR} is the influx of Ca^{2+} from ryanodine receptors (RyRs). Let

$[B_j]_T = ([B_j] + [CaB_j])$ be the total buffer concentration of jth buffer and the diffusion coefficient of buffer is not affected by the binding of calcium i.e., $D_{B_j} = D_{CaB_j}$. The Eq. (5) can be written as [17, 26]

$$R_j = -k_j^+ [Ca^{2+}][B_j] + k_j^- ([B_j]_T - [B_j]). \tag{6}$$

We assume that the buffer concentration is present in excess inside the cytosol so that the concentration of free buffer is constant in space and time i.e., $[B_j] \cong [B_j]_\infty$. Under this assumption Eq. (6) is approximated by [12, 17, 20, 26, 28]

$$k_j^+ [Ca^{2+}][B_j] \approx k_j^- ([B_j]_T - [B_j]_\infty) \tag{7}$$

where $[B_j]_\infty = \frac{k_j^- [B_j]_T}{(k_j^- + k_j^+ [Ca^{2+}]_\infty)}$ is the background buffer concentration. Thus for single mobile buffer species Eq. (2) can be written as [17, 18, 26]

$$\frac{\partial [Ca^{2+}]}{\partial t} = D_{Ca} \nabla^2 [Ca^{2+}] - k_j^+ [B_j]_\infty ([Ca^{2+}] - [Ca^{2+}]_\infty)$$
$$+ \sigma_{RyR} + \delta\sigma(r) \tag{8}$$

Here $[Ca^{2+}]$ is background calcium concentration. σ_{RyR} is the influx of calcium through ryanodine receptor channels which is given by [12, 17, 29]

$$\sigma_{RyR} = V_{RyR} P_o ([Ca^{2+}]_{ER} - [Ca^{2+}]) \tag{9}$$

We assume a single point source of Ca^{2+}, $\sigma(r)$ at $r = 0$; there are no sources for buffers and buffer concentration is in equilibrium with Ca^{2+} far from the source and ∇ is the Laplacian operator i.e., $\nabla^2 = \frac{\partial^2}{\partial r^2} + \frac{2}{r}\frac{\partial}{\partial r}$.

Combining Eqs. (8) and (9) we get the mathematical model as given below

$$\frac{\partial [Ca^{2+}]}{\partial t} = D_{Ca} \nabla^2 [Ca^{2+}] - k_j^+ [B_j]_\infty ([Ca^{2+}] - [Ca^{2+}]_\infty)$$
$$+ V_{RyR} P_o ([Ca^{2+}]_{ER} - [Ca^{2+}]) + \delta\sigma(r) \tag{10}$$

The T lymphocyte cell is assumed to be spherical in shape [8]. The Eq. (10) for a one dimensional unsteady state case in polar spherical coordinates is given by

$$\frac{\partial [Ca^{2+}]}{\partial t} = \frac{1}{r^2} \frac{\partial}{\partial r} \left(D_{Ca} r^2 \frac{\partial [Ca^{2+}]}{\partial r} \right)$$
$$- k_j^+ [B_j]_\infty ([Ca^{2+}] - [Ca^{2+}]_\infty)$$
$$+ V_{RyR} P_o ([Ca^{2+}]_{ER} - [Ca^{2+}]) + \delta\sigma(r) \tag{11}$$

The point source of calcium is assumed at $r = 0$ and as we move away from the source, the calcium concentration achieves its background value i.e. 0.1 μM. Thus the initial and boundary conditions for the above problem are [26, 27, 30].

The boundary conditions are given by

$$\lim_{r \to 0} \left(4\pi D_{Ca} r^2 \frac{\partial [Ca^{2+}]}{\partial r} \right) = \sigma \tag{12}$$

$$\lim_{r \to 5} [Ca^{2+}] = 0.1 \ \mu M \tag{13}$$

The initial condition is given by

$$[Ca^{2+}]_{t=0} = 0.1 \ \mu M \tag{14}$$

Our problem is to solve Eq. (11) along with Eqs. (12–14). For our convenience we write 'u' in lieu of $[Ca^{2+}]$. The Eq. (11) in discretized variational form is given by

$$I^{(e)} = \frac{1}{2} \int_{r_i}^{r_j} \left[r^2 \left(\frac{\partial u^{(e)}}{\partial r} \right)^2 + \alpha r^2 \left(u^{(e)} \right)^2 - 2\beta r^2 u^{(e)} + \frac{r^2}{D_{Ca}} \frac{\partial (u^{(e)})^2}{\partial t} \right]$$
$$\times dr + \psi^{(e)} \left(\frac{\sigma u^{(e)}}{4\pi D_{Ca}} \right)_{r=0} \tag{15}$$

where $\alpha = \frac{1}{D_{Ca}} \left(k_j^+ [B_j]_\infty + V_{RyR} P_o \right)$, $\beta = \frac{1}{D_{Ca}} \left(V_{RyR} P_o u_{ER} + k_j^+ [B_j]_\infty u_\infty \right)$, $\psi^{(e)} = 1$ for $e = 1$ and $\psi^{(e)} = 0$ for rest of the elements, where $e = 1, 2, 3, \ldots 50$. The shape function of concentration variation within each element is defined as:

$$u^{(e)} = c_1^{(e)} + c_2^{(e)} r \tag{16}$$

or

$$u^{(e)} = p^T c^{(e)} \tag{17}$$

where

$$p^T = [1 \ r] \tag{18}$$

and

$$c^{(e)^T} = \left[c_1^{(e)} \ c_2^{(e)} \right] \tag{19}$$

Substituting nodal conditions in Eq. (17), we get

$$\bar{u}^{(e)} = P^{(e)} \times c^{(e)} \tag{20}$$

where

$$\bar{u}^{(e)} = \begin{bmatrix} u_i \\ u_j \end{bmatrix}, \quad P^{(e)} = \begin{bmatrix} 1 & r_i \\ 1 & r_j \end{bmatrix} \tag{21}$$

From the Eq. (20), we have

$$c^{(e)} = R^{(e)} \times \bar{u}^{(e)} \tag{22}$$

where

$$R^{(e)} = P^{(e)^{-1}} \tag{23}$$

Substituting $c^{(e)}$ from Eq. (22) in (17), we get

$$u^{(e)} = p^T R^{(e)} \bar{u}^{(e)} \tag{24}$$

Now the integral $I^{(e)}$ can be written in the form

$$I^{(e)} = I_l^{(e)} + I_m^{(e)} - I_n^{(e)} - I_k^{(e)} + I_p^{(e)} \tag{25}$$

where

$$I_l^{(e)} = \frac{1}{2} \int_{r_i}^{r_j} r^2 \left(\frac{\partial u^{(e)}}{\partial r} \right)^2 dr \tag{26}$$

$$I_m^{(e)} = \frac{1}{2} \int_{r_i}^{r_j} \alpha r^2 \left(u^{(e)} \right)^2 dr \tag{27}$$

$$I_n^{(e)} = \int_{r_i}^{r_j} \beta r^2 u^{(e)} dr \tag{28}$$

$$I_k^{(e)} = \psi^{(e)} \frac{\sigma}{4\pi D_{Ca}} u^{(e)} \big|_{r=0} \tag{29}$$

$$I_p^{(e)} = \frac{1}{D_{Ca}} \frac{d}{dt} \int_{r_i}^{r_j} r^2 \left(u^{(e)} \right)^2 dr \tag{30}$$

Now, we extremize the integral $I^{(e)}$ w.r.t. each nodal calcium concentration u_i as given below

$$\frac{dI^{(e)}}{d\bar{u}^{(e)}} = \frac{dI_l^{(e)}}{d\bar{u}^{(e)}} + \frac{dI_m^{(e)}}{d\bar{u}^{(e)}} - \frac{dI_n^{(e)}}{d\bar{u}^{(e)}} - \frac{dI_k^{(e)}}{d\bar{u}^{(e)}} + \frac{dI_p^{(e)}}{d\bar{u}^{(e)}} = 0 \tag{31}$$

$$\frac{dI}{d\bar{u}} = \sum \bar{M}^{(e)} \frac{dI^{(e)}}{d\bar{u}} \bar{M}^{(e)^T} = 0 \tag{32}$$

where $\bar{M}^{(e)} = \begin{bmatrix} 0 & 0 \\ . & . \\ 1 & 0 \\ 0 & 1 \\ . & . \\ 0 & 0 \end{bmatrix}$, $\bar{u} = \begin{bmatrix} u_1 \\ u_2 \\ . \\ . \\ . \\ u_{51} \end{bmatrix}$

Assembling the integrals (25), we get

$$I = \sum_{e=1}^{50} I^{(e)} \tag{33}$$

This leads to a following system of linear differential equations

$$[A]_{51 \times 51} [\bar{u}]_{51 \times 1} + [C]_{51 \times 51} \left[\frac{\partial u}{\partial t} \right]_{51 \times 1} = [B]_{51 \times 1} \tag{34}$$

Here, $[\bar{u}] = [u_1 \ u_2 \ u_3 \ \ldots \ u_{51}]^T$, A and C are the system matrix and B is the system vector. A computer program has been developed in MATLAB 7.10 for the whole problem and executed on Intel(R) Core™ i3 CPU, 4.00 GB RAM, 2.40 GH$_z$ processor.

3 Results and Discussion

In this section, the numerical computations were performed using a "finite difference in time, finite element in space" using linear basis functions. The simulations reported here have been designed to investigate the intracellular calcium concentration in T lymphocytes in presence and absence of the parameters. Our simulations also reproduce the relative values of intracellular calcium in the measured time courses.

The numerical values of biophysical parameters used in the model are stated in the Table 1. [8, 12, 17, 18, 26, 29].

Figure 1 shows radial calcium concentration for different source amplitudes and $B = 25$ μM. The calcium concentration is maximum at $r = 0$ μM i.e., source and it decreases as we go away from the source up to $r = 5$ μM. It is observed that the calcium concentration is higher for higher values of source amplitudes.
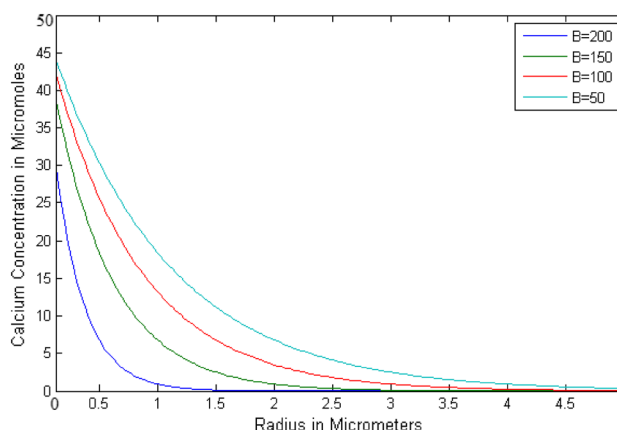
Figure 2 shows radial calcium concentration distribution for $\sigma = 1$ pA and different values of BAPTA buffer concentrations $B = 50, 100, 150$ and 200 μM. The calcium concentration is maximum at source i.e. $r = 0$. The peak value of calcium decreases with the increase in the buffer concentration. The gaps among the curves in Fig. 2 indicate that buffer has significant effect on calcium concentration distribution in the cell.

Figure 3 shows the radial calcium concentration distribution in presence and absence of RyR. It is observed that the presence of RyR raises the peak calcium concentration at the source $r = 0$. Further the gap between the curves indicates the effect of RyR on calcium concentration distribution in the cell.

Figure 4 shows the radial calcium concentration distribution due to the two different types of buffers namely BAPTA and EGTA buffers. The fall in the calcium concentration profiles for BAPTA buffer is sharper as compared to that for EGTA buffer. This is because the BAPTA
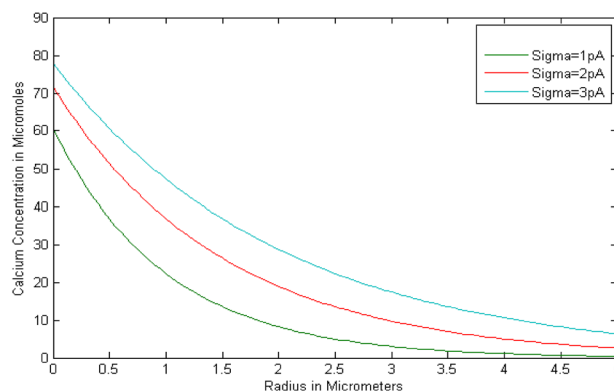
Fig. 1 Radial variation of calcium concentration for different source amplitudes i.e., $\sigma = 1$ pA, 2 pA, 3 pA, B = 25 μM

Fig. 2 Radial variation of calcium concentration for $\sigma = 1$ pA for different concentration of BAPTA buffer i.e., $B = 50, 100, 150, 200$ μM

buffer is a fast buffer and binds the calcium ions at faster rate than the EGTA buffer.

Figure 5 shows that the temporal variation of Ca^{2+} concentration in T lymphocytes for different concentrations of buffer. The effect of changing buffer concentration is clear in this figure. We observe that calcium concentration reaches steady state in less than 1000 ms. The peak value of Ca^{2+} concentration is different for different values of buffer concentration. The peak value of Ca^{2+} concentration is higher for lower concentration of buffer. It is also observed that the steady state is achieved early for higher buffer concentration. The reason for this is that the higher concentration of buffers binds more calcium and then forcing the system to reach steady state early.
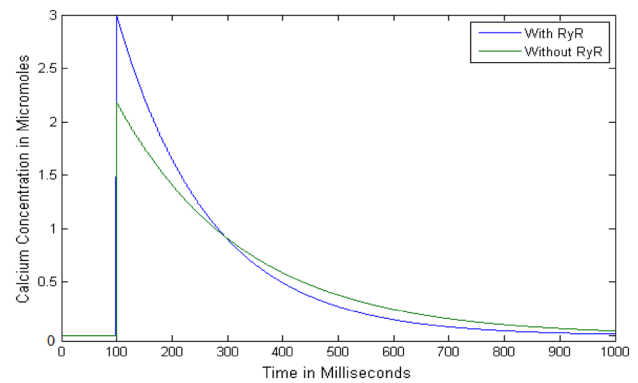
Figure 6 shows temporal variation of Ca^{2+} concentration in T lymphocytes in presence and absence of Ryanodine Receptor Ca^{2+} channel. It is observed that Ca^{2+} concentration is lower in absence of Ryanodine receptor. The figure further shows that the Ca^{2+} concentration is higher in presence of the receptor as receptor releases the Ca^{2+} thus

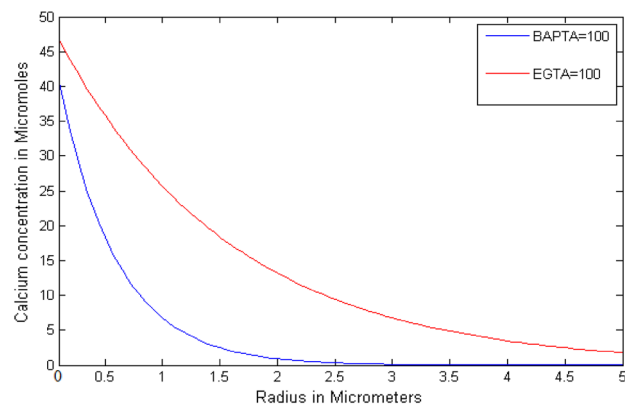**Table 1** Values of biophysical parameters [8, 12, 17, 26, 29]

| Symbol	Parameter	Value
D_{Ca}	Diffusion coefficient	250 μM²/s
k_j^+	On rate for EGTA	3/μM s
k_j^-	Off rate for EGTA	1/s
k_j^+	On rate for BAPTA	100/μM s
k_j^-	Off rate for BAPTA	10/ s
$[B_j]_\infty$	Total buffer concentration	100 μM
σ	Source amplitude	1 pA
V_{RyR}	RyR receptor rate	0.5 μM/s
$[Ca^{2+}]_{ER}$	Calcium concentration of ER	400 μM
P_o	Rate of calcium efflux	0.5 M/s
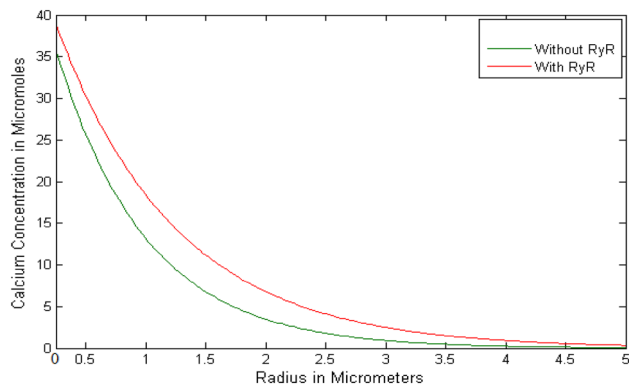
Fig. 3 Radial variation of calcium concentration for $\sigma = 1$ pA in presence and absence of RyR

Fig. 4 Radial variation of calcium concentration for two different types of buffers EGTA $= 100$ μM and BAPTA $= 100$ μM, $\sigma = 1$ pA
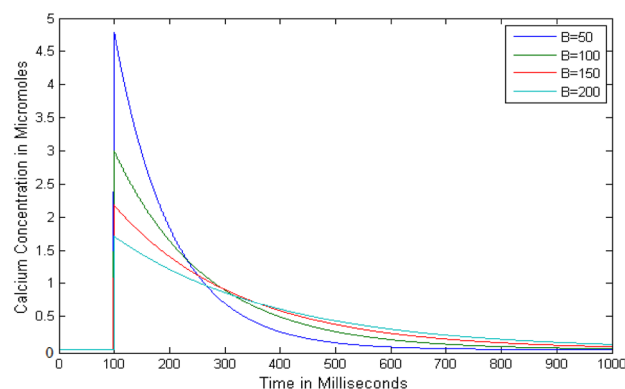
Fig. 5 Temporal variation of calcium concentration in T lymphocytes for different concentrations of Buffers i.e., B $= 50$, 100, 150, 200 μM

Fig. 6 Temporal variation of calcium concentration in T lymphocytes in the presence and absence of ryanodine receptor

The Ca^{2+} concentration is higher at 100 ms after that it decreases rapidly and becomes almost steady at 800 ms.

The results obtained here are in agreement with the biological facts. But no such experimental results are available for comparison. Similar results have been observed in other cells like neuron cells, astrocytes, oocytes etc. [10–24] and our results are in agreement with them.

4 Conclusion

The proposed finite element model has been employed successfully to study the relationships of spatial–temporal calcium concentration distribution with buffers, source amplitude, RyR etc. in T lymphocytes. From the results it can be concluded that the source amplitude, buffers and RyR have significant impact on calcium concentration distribution patterns in T lymphocytes required for maintaining the structure and function of the cell. Such models can be developed further to get deeper insights of calcium concentration regulation mechanism in T lymphocytes and generate information which can be useful to biomedical scientists for developing protocols for diagnosis and treatment of diseases associated with T lymphocytes.

causes increase in Ca^{2+} concentration. The Ca^{2+} concentration is higher from $t = 100$ ms to $t = 500$ ms and then remains in steady state. The Ca^{2+} concentration in presence of ryanodine receptor is maximum and reaches up to 3 μM.

References

1. Toldi G (2013) The regulation of Calcium homeostasis in T lymphoctes. Front Immunol. doi:10.3389/fimmu.2013.00432
2. Kummerow C, Junker C, Kruse K, Rieger H, Quintana A, Hoth M (2009) The immunological synapse controls local and global calcium signals in T lymphocytes, vol 231. John Wiley & Sons, Hoboken, pp 132–147

3. Cahalan MD, Chandy KG (2009) The functional network of ion channels in T lymphocytes. Immunol Rev 231:59–87
4. Feske S, Skolnik EY, Prakriya M (2012) Ion channels and transporters in lymphocyte function and immunity. Nat Rev Immunol 12:532–547
5. Tsaneva-atanasova K, Shuttle worth TJ, Yule DI, Thompson JL, Sneyd J (2005) Calcium oscillations and membrane transport. The important of two time scales. Multiscale Model Simul 3(2):245–264
6. Neher E (1986) Concentration profiles of intracellular Ca^{2+} in the presence of diffusible chelator. Exp Brain Res 14:80–96
7. Tang Y, Schlumpberger T, Kim T, Lueker M, Zucker RS (2000) Effects of mobile buffers on facilitation: experimental and computational studies. Biophys J 78:2735–2751
8. Schmeitz C, Hernandez-Vargas EA, Fliegert R, Guse AH, Hermann MM (2013) A mathematical model of T lymphocyte calcium dynamics derived from single transmembrane protein properties. Front Immunol. doi:10.3389/fimmu.2013.00277
9. Ernst IMA, Fliegert R, Guse AH (2013) Adenine dinucleotide second messengers and T lymphocyte calcium signaling. Front Immunol 4:259. doi:10.3389/fimmu.2013.00259
10. Hou P, Zhang R, Liu Y, Feng J, Wang W, Wu Y, Ding J (2014) Physiological role of Kv1.3 channel in T Lymphocyte cell investigated quantitatively by kinetic modeling. doi:1371/journal.pone.0089975
11. Smith GD (1996) Analytical steady state solution to the rapid buffering approximation near an open Ca^{2+} channel. Biophys J 71:3064–3072
12. Tewari S, Pardasani KR (2008) Finite difference model to study the effects of Na^+ influx on cytosolic Ca^{2+} diffusion. WorldAcademy of Science, Engineering and Technology, vol 15, pp 670–675
13. Tewari S, Pardasani KR (2010) Finite element model to study two dimensional unsteady state cytosolic calcium diffusion in presence of excess buffers. IAENG Int J Appl Math 40:3
14. Tripathi A, Adlakha N (2011) Finite volume model to study calcium diffusion in neuron involving J_{RyR}, J_{SERCA}, and J_{LEAK}. J Comput 3(11) ISSN 2151-9617
15. Tripathi A, Adlakha N (2011) Finite volume model to study calcium diffusion in neuron cell under excess buffer approximation. Int J Math Sci Eng Appl 5:1816–1838
16. Tripathi A, Adlakha N (2012) Two dimensional coaxial circular elements in FEM to study calcium diffusion in neuron cells. Appl Math Sci 6(10):455–466
17. Jha BK, Adlakha N, Mehta MN (2010) Finite volume model to study the effect of buffer on cytosolic Ca^{2+} advection diffusion. Int J Eng Nat Sci 4(3):160–163
18. Jha BK, Adlakha N, Mehta MN (2012) Analytic solution of two dimensional advection diffusion equation arising in cytosolic calcium concentration distribution. Int Math Forum 7(3):135–144
19. Naik PA, Pardasani KR (2013) One dimensional finite element method approach to study effect of ryanodine receptor and serca pump on calcium distribution in oocytes. J Multiscale Model 5(2):1–13
20. Naik PA, Pardasani KR (2013) Finite element model to study effect of buffers in presence of voltage gated Ca^{2+} Channels on calcium distribution in oocytes for one dimensional unsteady state case. Int J Modern Biol Med 4(3):190–203
21. Naik PA, Pardasani KR (2014) Finite element model to study effect of Na^+/K^+ pump and Na^+/Ca^{2+} exchanger on calcium distribution in oocytes in presence of buffers. Asian J Math Stat 7(1):21–28
22. Panday S, Pardasani KR (2013) Finite element model to study effect of buffers along with leak from ER on cytosolic Ca^{2+} distribution in oocyte. IOSR J Math (IOSR-JM) ISSN: 2278–5728. 4(5) PP01-08
23. Panday S, Pardasani KR (2013) Finite element model to study effect of advection diffusion and Na^+/Ca^{2+} exchanger on Ca^{2+} distribution in oocytes. J Med Imaging Health Inform 3:374–379
24. Panday S, Paradasani KR (2014) Finite element model to study the mechanics of calcium regulation in oocyte. J Mech Med Biol. doi:10.1142/S0219519414500225
25. Manhas N, Sneyd J (2014) Pardasani KR Modelling the transition from simple to complex Ca^{2+} oscillations in pancreatic acinar cells. J Biosci 39(3):463–484
26. Kotwani M, Adlakha N, Mehta MN (2012) Numerical model to study calcium diffusion in fibroblasts cell for one dimensional unsteady state case. Appl Math Sci Hikari 6(102):5063–5072
27. Leena S (2014) A numerical model to study the rapid buffering approximation near an Open Ca^{2+} channel for an unsteady state case. World Acad Sci Eng Technol Int J Math Comput Phys Quant Eng 8(2):445–449
28. Naik PA, Pardasani KR (2015) One dimensional finite element model to study calcium distribution in oocytes in presence of VGCC, RyR and buffers. J Med Imaging Health Inform 5(3):471–476
29. Tiwari S (2009) A variational-ritz approach to study cytosolic calcium diffusion in neuron cells for a one dimensional unsteady state case. GAMS J Math Math Biosci 2:1–10
30. Smith GD, Dai L, Miura RM, Sherman A (2000) Asymptotic analysis of buffered calcium diffusion near a point source. SIAM J Appl Math 61:1816–1838